Desalination and Water Treatment
www.deswater.com

doi: 10.5004/dwt.2019.23774

150 (2019) 310–319
May

Degradation of phthalic acid esters by zero-valent iron and persulfate using bacth experiments at different temperatures

Muhammad A. Imran, Yuzhen Tong, Yifan Ding, Mingzhu Liu*, Honghan Chen

Beijing Key Laboratory of Water Resources & Environmental Engineering, China University of Geosciences (Beijing), Beijing, China, Tel. +86-10-82322332; Fax: +86-10-82321081; email: liumz@cugb.edu.cn (M. Liu), Tel. +86-15-650767107; email: alimalik2217@yahoo.com (M.A. Imran), Tel. +86-18-800167566; email: 729551561@qq.com (Y. Tong), Tel. +86-18-614063965; email: yfding326@hotmail.com (Y. Ding), Tel. +86-86-82323345; email: chenhh@cugb.edu.cn (H. Chen)

Received 28 August 2018; Accepted 10 January 2019

ABSTRACT

Phthalic acid esters (PAEs) are often detected in groundwater. Degradation of PAEs in groundwaters is more difficult than in surface waters because of their lower temperatures. Degradation of three PAEs (di(2-ethylhexyl) phthalate (DEHP), dibutyl phthalate (DBP), and dimethyl phthalate (DMP)) were investigated in ZVI-persulfate system at 15°C, 20°C, 25°C, and 30°C. Degradation rates of these PAEs were much faster when persulfate was activated by ZVI in comparison with the persulfate activated by heat only. PAEs degradation slowed down as temperature decreased. Degradation of DEHP, DBP, and DMP at 15°C in 180 min was 32%, 47%, and 5%, respectively. PAEs with longer carbon chains degraded more than PAEs with shorter carbon chains at 25°C–30°C. Conversion of persulfate into sulfate, release of iron ions, and variation in pH values in the solutions were also investigated. Persulfate ions consumption and dissolution of iron ions increased as temperature increased. About 47–57 mg/L of sulfate ions formed from 60 mg/L of persulfate. pH values remained in the 3.5–4. range. Our work provides basic and guidance knowledge for in situ PAEs remediation from groundwaters.

Keywords: PAEs; Zero-valent iron; Persulfate; Temperature; Batch test

1. Introduction

Extensive use of phthalate acid esters (PAEs) in a wide range of commercial and industrial products (such as cosmetics, polyvinyl chloride, cellulose, rubber, styrene, etc.) led to the ubiquitous presence of these toxic and xenobiotic compounds in the environment [1–5]. Exposure to PAEs and their by-products might cause carcinogenic and estrogenic side-effects as well as adverse damage of the reproduction systems [6–8]. Children are even more prone to the harmful effects associated with exposure to PAEs [9], thus, presence of PAEs in the environment cannot be ignored.

Di(2-ethylhexyl) phthalate (DEHP), dibutyl phthalate (DBP), and dimethyl phthalate (DMP) are the most common and extensively used PAEs [10–12]. Because they are toxic, slowly degrade, and hydrolyze in natural conditions, United State Environmental Protection Agency (US EPA) and China National Environmental Monitoring Centre (CNEMC) [13] included PAEs into priority pollutant list.

PAEs contaminate surface waters during domestic and industrial run-offs. Surface waters eventually pass this contamination to soil and groundwaters [14–16]. All PAEs on this priority pollutant list were detected in groundwaters of North China [17]. A lot of research was conducted to study different methods to remove PAEs. One of such methods is advance oxidation methods such as photocatalytic oxidation [18–20], ozone oxidation [21], UV photolysis [22–23], and Fenton oxidation [24]. These techniques effectively decompose PAEs but with certain limitations. For example, UV photolysis and photocatalytic oxidation typically cannot be applied to in situ groundwater treatments. Hydrogen

---

* Corresponding author.

1944-3994/1944-3986

peroxide (H_2O_2) cannot be distributed quick enough to avoid its degradation before it reaction with PAEs [25]. Ozone (O_3) has limited solubility diffuses and distributes poorly in the subsurface environment. Its on-site synthesis in large quantities is also a drawback [26].

Recently, ZVI-persulfate system, based on the activation of persulfate ion ($S_2O_8^{2-}$)by zero-valent iron (ZVI), showed efficient destruction of a wide range of pollutants, such as 1,4-dioxane [27], p-chloroaniline [28], bentazon [29], rhodamine B [30], unsymmetrical dimethylhydrazine [31], etc. Persulfate is a well-known strong and stable oxidant, which is easy to handle and apply in the field. It has a long life and large area of influence in subsurface systems [32]. Conversion of persulfate to sulfate radicals can be achieved by simple methods, such as heat, UV, microwaves, and treatment with transition metal ions [33–34]. Persulfate activation with ZVI has a lot of more advantages comparing with these methods: ZVI is efficient, cost effective, and non-toxic [35]. ZVI is also a slow releasing source of Fe^{2+}, which can assist in sulfate radical formation (see Eqs. (1) and (2)). Schematics of basic reaction for the persulfate activation by ZVI to generate sulfate radical and Fe^{2+} is presented in Fig. 1.

$$Fe^{o} + S_2O_8^{2-} \rightarrow Fe^{2+} + SO_4^{2-} \tag{1}$$

$$Fe^{2+} + S_2O_8^{2-} \rightarrow Fe^{3+} + SO_4^{-} + SO_4^{2-} \tag{2}$$

Studies on degradation of PAEs by persulfate and ZVI-persulfate systems are limited. For example, one study [36] reported degradation of DMP with persulfate activated by heat only. In another study, degradation of DBP was investigated at different pH values [37]. Typically, more than one PAE coexist in the same proximity, therefore, comparative rates of degradation as function of carbon chain size by the same chemical oxidants are important to investigate. The main objectives of this work are to: (1) investigate degradation behavior of PAEs in ZVI-persulfate system; and to (2) analyze PAE degradation rate at 15°C–30°C with respect to their carbon chain size. To understand consumption of persulfate ions, release of ferrous ion (Fe^{2+}) and pH changes were measured as well. Our ultimate goal is to provide foundation for in situ chemical oxidation methodology (such as permeable reactive barriers) and explore its applicability in removal of ester contaminants from reclaimed water to replenish groundwater.

2. Materials and methods

DEHP (99.5%), DMP (99.5%), DBP (99.5%), and sodium persulfate (99%) of analytical grade as well as acetonitrile and methanol (both of HPLC grade) were purchased from Tianjin Fuchen Chemical Reagent Co. (Tianjin, China). ZVI was ground and passed through a 0.25 μm sieve, after which it was treated for 10 min with 0.5 M HCl and rinsed with ultra–pure water till pH of the solution became 7. Prepared ZVI samples were freeze-dried and stored in anaerobic condition. The ultra-pure water was prepared using Millipore Milli-Q system.

The batch reactions were conducted in 40 ml brown glass bottles with rubber stoppers using rotary shaker at 180 rpm and different temperatures (15°C, 20°C, 25°C, and 30°C). Details of this methodology and basic reactions between ZVI and persulfate are shown in Fig. 1. Three individual 5 mg/L solutions of DEHP, DMP, and DBP were prepared in methanol. For all reactions, 0.4 g/L solution of ZVI and 60 mg/L solution of persulfate were used. Batch reactions started when predetermined amount of sodium persulfate and 0.016 g of ZVI was added to each PAE solution. Samples were analyzed at certain time intervals and centrifuged at 1,500 rpm for 5 min

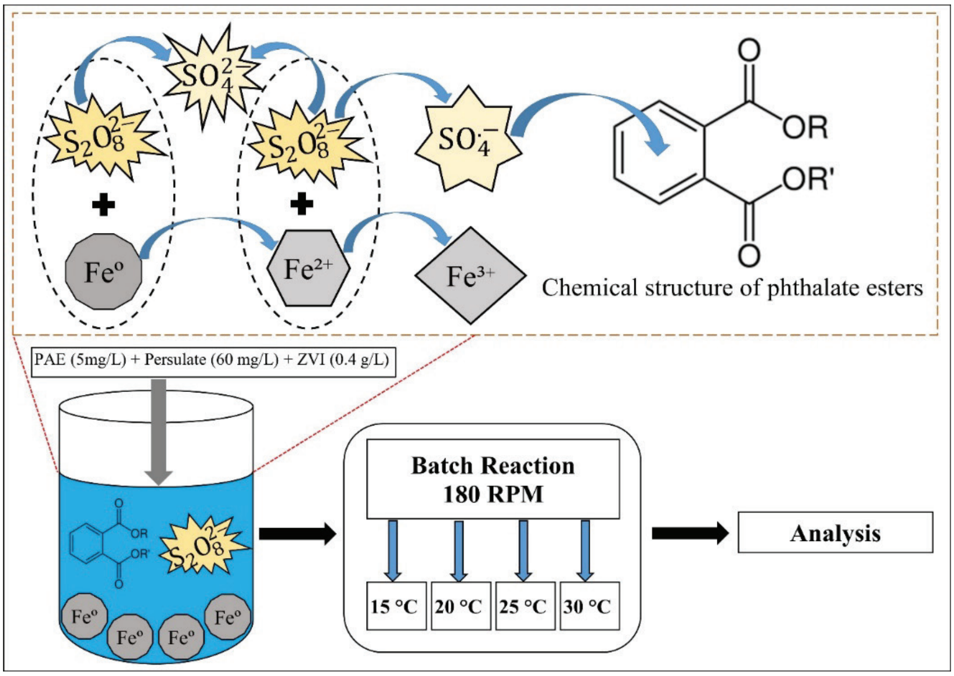

Fig. 1. Schematics of experiment methodology and basic reaction between ZVI and persulfate.

to separate solutions from the residual ZVI. The supernatant was decanted and analyzed to determine PAE contents. Samples were not filtered for PAEs analysis to avoid accumulation of PAEs on the filter membranes. PAEs concentration at each interval was marked as (C_t), which was used to calculate PAE removal efficiency (Eq. (3)). Kinetic parameters of PAEs degradation were estimated using Eq. 4(a). Results of this calculation were plotted as logarithmic function (Eq. 4(b)). Each sample was passed through 0.45 μm polytetrafluoroethylene (PTFE) membrane before analysis of persulfate and sulfate ions as well as total dissolved iron, ferrous ion and pH. All the batch reactions were performed in duplicates. To determine PAEs contents more precisely, two different samples were analyzed from each batch. Control samples containing no persulfate and no ZVI were analyzed as well to determine PAEs evaporation losses.

$$\text{Removal efficiency}\left(\%\right) = \left(1 - \frac{C_t}{C_o}\right) \times 100 \tag{3}$$

$$C_t = C_o e^{(-kt)} \tag*{4(a)}$$

$$\ln C_t = \ln C_o - kt \tag*{4(b)}$$

Concentration of DEHP, DBP, and DMP were obtained using high performance liquid chromatography (HPLC-UV, Agilent 1200 series) equipped with a reverse phase ZORBAX SB–Aq column (150 mm × 4.6 mm, 5 μm). A mixture of acetonitrile and water was used as a mobile phase with volume ratios equal to 90:10, 70:30, and 60:40 for analyses of DEHP, DBP, and DMP, respectively. Oven temperature for DEHP was 35°C and 30°C for DBP and DMP. The wavelength of the UV detector was 230 nm for DBP and 228 nm for DEHP and DMP. The eluent flow rate (equal to 1 mL/min) and injection volume (equal to 20 μL) were the same for all PAEs. Summary of analysis conditions are shown in Table 1.

Concentration of sulfate ions (SO_4^{2-}) was measured using DR-6000 spectrophotometer based on the SulfaVer4 method, which is equivalent to USEPA turbidimetric method 375.4 for wastewater. Persulfate ($S_2O_8^{2-}$) ions were analyzed spectrophotometrically at 400 nm using potassium iodide (KI) [38]. Concentration of ferrous ions (Fe^{2+}) was determined by a spectrophotometer at 510 nm after adding 1, 10-phenanthroline. Concentration of total dissolved iron was determined by analyzing ferric ion (Fe^{3+}) content using hydroxylamine hydrochloride. For this purpose, all ferrous ions (Fe^{2+}) were oxidized to ferric ions.

3. Results and discussion

3.1. Degradation of di(2-ethylhexyl) phthalate

Neutralization of DEHP by combination of persulfate and ZVI at 15°C, 20°C, 25°C, and 30°C are shown in Fig. 2. Degradation of DEHP accelerated as temperature increased. Degradation of DEHP equal to ~32% was observed at 15°C after 180 min. At other temperatures, DEHP was 40% (at 20°C), 62% (at 25°C), and 73% (at 30°C). DEHP degradation rate at 15°C reduced by >50% as compare with 30°C. Plot reflecting remaining concentration ([DEHP]/[DEHP]o) as a function of the reaction time was fitted with pseudo-first-order model. Kinetic equation and half-life ($t_{1/2}$) of DEHP degradation are shown in Table 2. The first-order kinetic rate constants (k_{obs}) were calculated to be 2.1×10^{-3} (with correlation coefficient R^2 equal to 0.9622), 2.8×10^{-3} ($R^2 = 0.9895$), 55.0×10^{-3} ($R^2 = 0.9982$) and 7.9×10^{-3} ($R^2 = 0.9844$) min^{-1} at 15°C, 20°C, 25°C, and 30°C, respectively. Values of k_{obs} increased as the temperature increased. These results agree well with previously reported ones: for example, that destruction of polyvinyl alcohol accelerated as temperature increased [39], or that high temperatures benefited oxidation of bentazon in the ZVI–persulfate system [29]. Thus, DEHP degradation was much better at higher temperatures (25°C–30°C) than at lower temperatures (15°C–20°C).

Previous studies [28,36] described that the degradation of organic pollutants accelerates at higher temperatures because more sulfate radicals are produced, which results in higher consumption rate of persulfate. Therefore, we also compared consumption of persulfate as function of the sulfate ion generation at different temperatures. Decomposition of persulfate into sulfate ions during DEHP degradation as function of reaction time is shown in Figs. 3(a)–(d). Oxidation

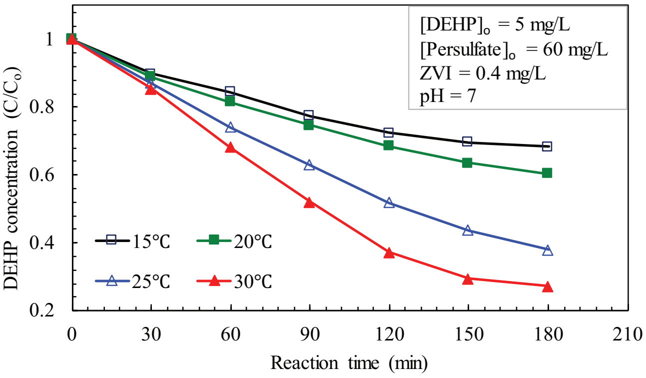

Fig. 2. Effect of the reaction temperature on DEHP degradation.

Table 1
HPLC conditions and peak time for DEHP, DBP and DMP

PAEs	Chemical formula	Mobile phase (acetonitrile –water) volume ratio	Flow rate (mL/min)	Injection volume (μL)	Temperature (°C)	Wavelength (nm)	Peak time (min)
DEHP	$C_{24}H_{38}O_4$	90:10	1	20	35	228	3.9
DBP	$C_{16}H_{22}O_4$	70:30	1	20	30	230	4.0
DMP	$C_{10}H_{10}O_4$	60:40	1	20	30	228	2.9

of persulfate was faster as reaction temperature increased. However, total conversion of persulfate into sulfate ions was ~80% after 180 min at all temperatures. Persulfate conversion to sulfate was almost linear at 15°C and 20°C. About 30 mg/L of persulfate (which corresponds to ~50% of its initial concentration) decomposed during the first 90 min (see Figs. 3(a) and (b)). However, an abrupt oxidation of persulfate occurred at the beginning of the reaction at higher temperatures: ~33 and ~30 mg/L (which correspond to ~50% of the initial concentration) of persulfate remained at 25°C and 30°C after the first 30 min, respectively (see Figs. 3(c) and (d)).

Dissolution of ZVI in the aqueous solution in term of total dissolved iron and Fe^{2+} along with variation in pH at different temperatures is shown in Figs. 4(a)–(d). Maximum concentration of Fe^{2+} (equal to 11.46 mg/L) was at 30°C after 120 min. At 20°C and 25°C, concentration of Fe^{2+} was insufficient. At the same time, at 15°C, Fe^{2+} concentration reached 6.36 mg/L. pH values decreased rapidly within the 30 min of the reaction, after which they remained stable. pH values ranged from 3.53 to 3.96 at all temperatures. pH value decreased because more H^+ formed during Fe^0/Fe^{2+} reaction according to Eqs. (5) and (6) [36]. Additionally, pH values could decrease because of Fe^{2+} hydrolysis and a consequent release of H^+ from bisulfate ion (HSO_4^-)) (Eqs. (7)–(10)) [40].

$$3Fe^{2+} + 4H_2O \rightarrow Fe_3O_4 + 8H^+ + 2e^- \quad (5)$$

$$3Fe^{o} + 4H_2O \rightarrow Fe_3O_4 + 8H^+ + 8e^- \quad (6)$$

$$Fe^{3+} + 3H_2O \rightarrow Fe(OH)_3 + 3H^+ \quad (7)$$

$$2S_2O_8^{2-} + 2H_2O \rightarrow 4HSO_4^- + O_2 \quad (8)$$

$$SO_4^{-} + H_2O \rightarrow OH + HSO_4^- \quad (9)$$

$$HSO_4^- \rightarrow SO_4^{2-} + H^+ \quad (10)$$

3.2. Degradation of dibutyl phthalate

DBP showed a rapid degradation during the first 30 min, after which it degraded linearly at a relatively slow rate (see Fig. 5). 28%–33% of the initial DBP decomposed within the first 30 min. Total degradation of DBP after 180 min ranged from 47% to 58%. An efficient degradation of DBP equal to ~47% was observed at 15°C. On the other hand, DBP is

Table 2
Kinetic parameters of DEHP and DBP degradation at different temperatures

Temperature (°C)	DEHP		DBP	
	Kinetic equations	$t_{1/2}$ (min^{-1})	Kinetic equations	$t_{1/2}$ (min^{-1})
15	$\text{In}C_t = -0.0021t - 0.0348$	330	$\text{In}C_t = -0.0030t - 0.1525$	231
20	$\text{In}C_t = -0.0028t - 0.0261$	248	$\text{In}C_t = -0.0032t - 0.1589$	217
25	$\text{In}C_t = -0.0055t + 0.0180$	126	$\text{In}C_t = -0.0036t - 0.1670$	193
30	$\text{In}C_t = -0.0079t + 0.0385$	88	$\text{In}C_t = -0.0041t - 0.1654$	169

Note: Kinetic parameters for DMP could not be determined because of insufficient reaction time and degradation.

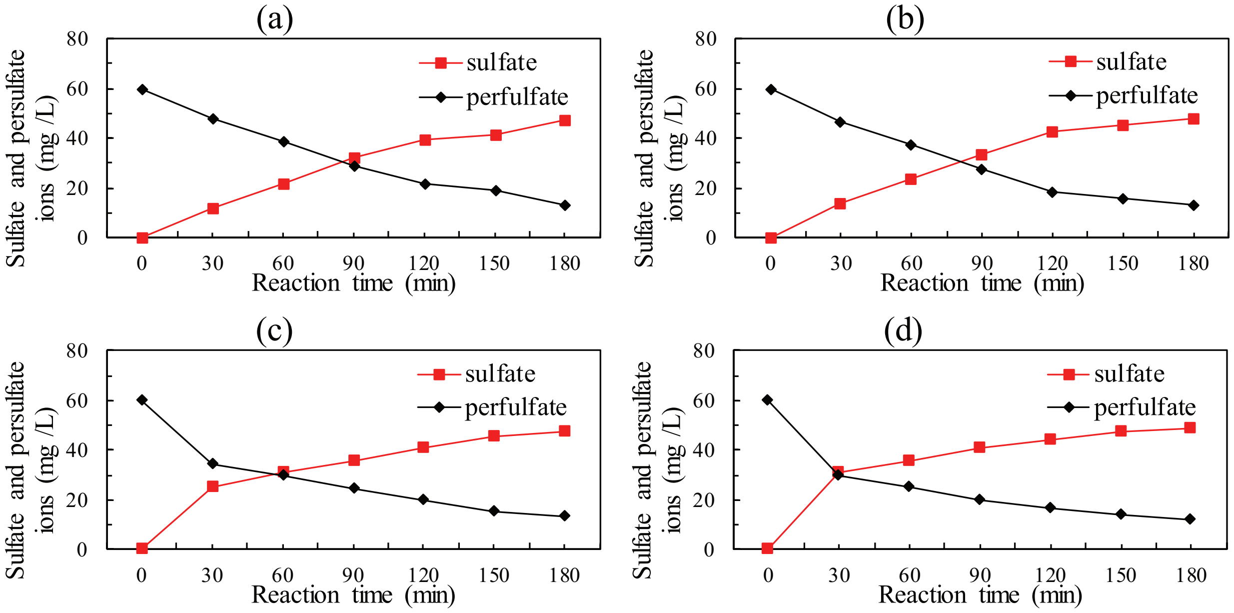

Fig. 3. Conversion of persulfate into sulfate during DEHP tests at (a) 15°C, (b) 20°C, (c) 25°C, and (d) 30°C.

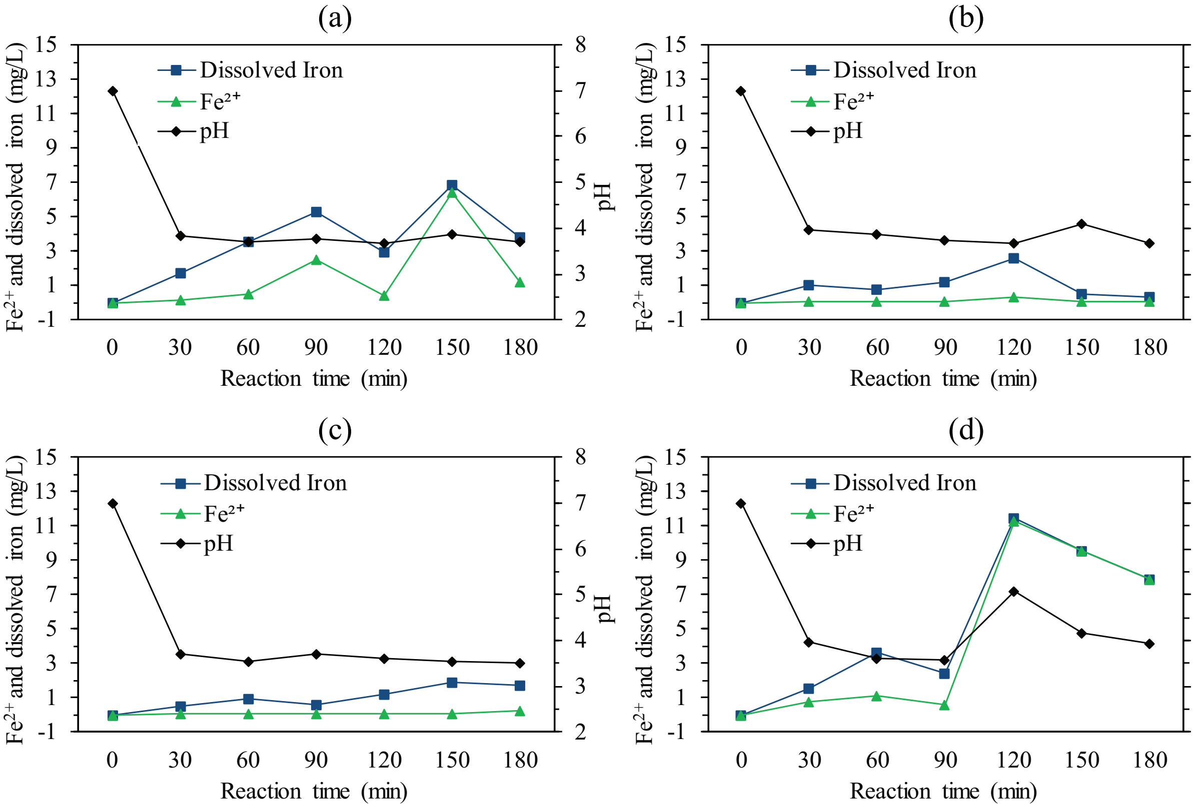

Fig. 4. Iron ions concentrations and pH during DEHP decomposition at (a) 15°C, (b) 20°C, (c) 25°C, and (d) 30°C.

the leading PAE contaminate in the groundwaters of north China according to the study of [17]. Thus, effective removal of DBP from groundwater can be achieved by ZVI-persulfate technology.

Kinetic parameters of DBP degradation are listed in Table 2, which show a good fit to the pseudo-first-order model. Rate constants (k_{obs}) are equal to 3.0×10^{-3} (with the correlation coefficient R^2 equal to 0.8360), 3.2×10^{-3} ($R^2 = 0.8443$), 3.6×10^{-3} ($R^2 = 0.8629$) and 4.1×10^{-3} ($R^2 = 0.8936$) min^{-1} at 15°C, 20°C, 25°C, and 30°C, respectively. Although the difference in DBP degradation between 15°C and 30°C was small comparing with DEHP degradation, we still observed positive effect of temperature on DBP degradation. Our results agree with the previously reported experiments [37], in which DBP decomposition was performed in ZVI-persulfate system at pH = 7 and at 25°C.

Conversion of persulfates into sulfate ions as function of the reaction time during DBP batch tests is shown in Figs. 6(a)–(d). More persulfate was consumed as reaction temperature increased. DBP degradation was fast at the beginning of the reaction, thus, persulfate was also consumed rapidly. Almost 50 mg/L of sulfate was obtained after 60 min of reaction at all temperatures. After 60 min, persulfate consumption slowed down. The total consumption of persulfate at 15°C, 20°C, 25°C, and 30°C was 52.2, 55.7, 57.1, and 57.1 mg/L, respectively.

Concentration of total dissolved iron, Fe^{2+} and pH variations during DBP batch experiments are shown in (Figs. 7(a)–(d)). Total dissolved iron and Fe^{2+} either increase linearly with reaction time or spiked and then decreased. The highest concentration of Fe^{2+} was 12.74, 6.9, 10.4, and 12.53 mg/L at 15°C, 20°C, 25°C, and 30°C. Thus, Fe^{2+} was available at all temperatures to assist persulfate decomposition. More Fe^{3+} formed at the beginning of the reaction and at lower temperatures (see Figs. 6(a) and (b)). After 2 h, concentration of Fe^{2+} became equal to the total dissolved iron content, which can be explained by secondary reaction involving Fe^{3+} (Eq. (11)) [41].

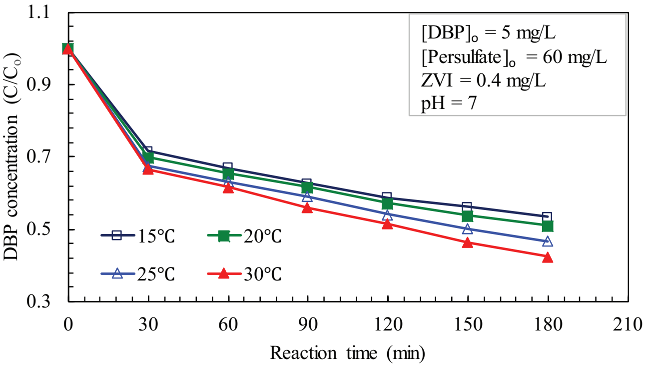

Fig. 5. DBP concentration change as function of the temperature.

$$Fe^{o} + 2Fe^{3+} \rightarrow 3Fe^{2+} \quad (11)$$

pH values were mostly in 3.4–3.7 range. Unusually high pH values were noticed for samples containing the highest Fe^{2+} concentrations, which can be explained by formation

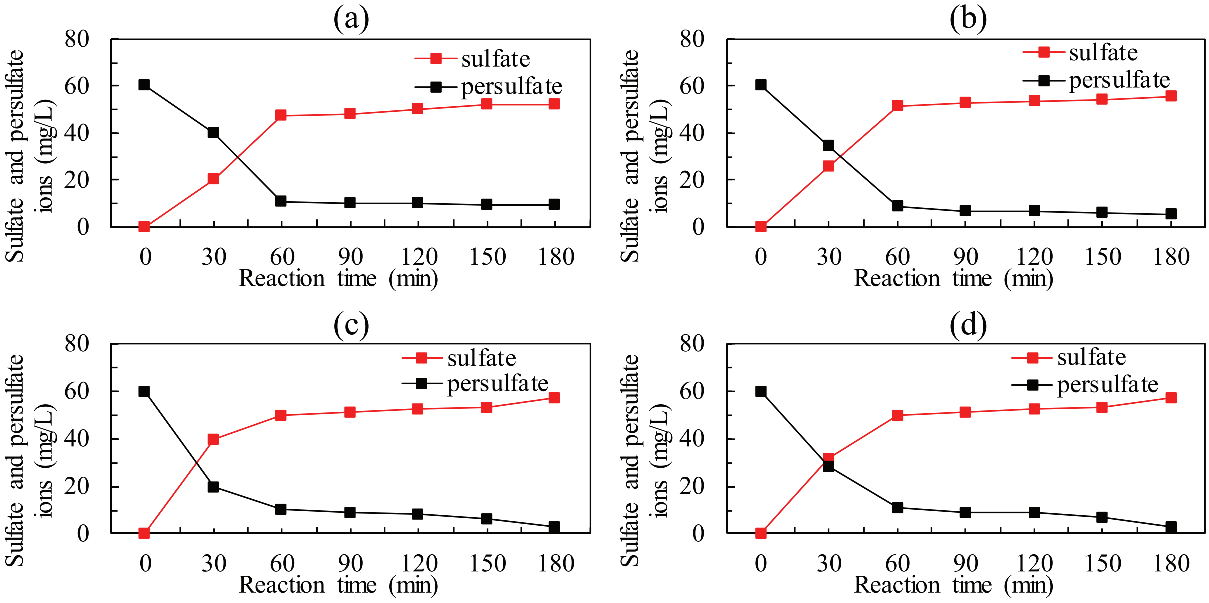

Fig. 6. Conversion of persulfate into sulfate during DBP tests at (a) 15°C, (b) 20°C, (c) 25°C, and (d) 30°C.

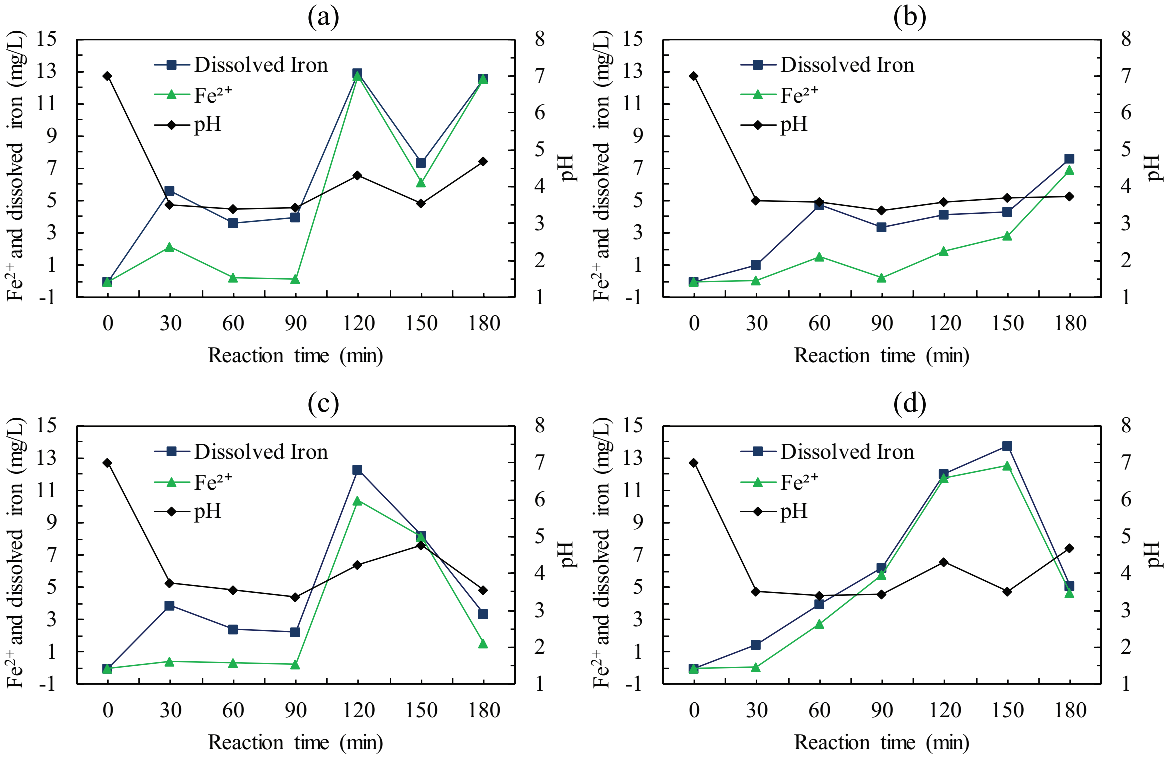

Fig. 7. Iron concentration and pH values during DBP decomposition at (a) 15°C, (b) 20°C, (c) 25°C, and (d) 30°C.

of hydroxide ions both in aerobic and anaerobic conditions (Eqs. (12) and (13)) [39].

Aerobic conditions: $\mathrm{Fe^{o} + H_2O + 0.5O_2 \rightarrow Fe^{2+} + 2OH^{-}}$ (12)

Anaerobic conditions: $\mathrm{Fe^{o} + H_2O \rightarrow Fe^{2+} + 0.5H_2 + 2OH^{-}}$ (13)

3.3. Degradation of dimethyl phthalate

DMP decomposition in the ZVI-persulfate system at various temperatures is shown in Fig. 8. Noticeable oxidation of DMP started at ~150 min reaction time. Maximum DMP degradation (equal to 15%) was observed at 30°C after 3 h. This is somewhat agrees with previous reports [36], in which ~44% DMP was decomposed by persulfate at 30°C after 48 h.

However, DMP decomposition in the ZVI-persulfate system is much faster comparing with the reaction activated by heat only. Reaction kinetics of DMP degradation could not determined with more details as the reaction time was short. Thus, complete degradation of DMP in ZVI-persulfate system still needs to be studied.

Total consumption of persulfate was ~49, 50, 51, and 53 mg/L at 15°C, 20°C, 25°C, and 30°C, respectively (Figs. 9(a)–(d)). Persulfate consumption during the first 30 min was ~20 mg/L at 15°C–20°C and ~40 mg/L at 25°C–30°C. This experiment also showed rapid and high quantity production of sulfates ions from persulfates at higher temperatures. Concentration of Fe^{2+} increased almost linearly at 15°C and showed maximum value equal to 11.44 mg/L at 180 min. At 25°C–30°C, concentration of released Fe^{2+} reached its maximum and then decreased. Maximum Fe^{2+} concentration reached 11.45, 9.20, and 13.20 mg/L at 20°C, 25°C, and 30°C, respectively (Figs. 10(a)–(d)). Possible reasons for higher Fe^{2+} concentrations are reduction of Fe^{3+} to Fe^{2+} according to Eq. (11) as well as continuous Fe^{2+} formation from ZVI (Eq. (1)). More Fe^{3+} formed at the beginning of the reaction and at lower temperatures. pH values were in the 3.34–3.78 range except for the samples with high concentration of Fe^{2+}. Maximum pH values equal to 3.99 (after 180 min), 4.57 (after 120 min), 4.00 (after 180 min), and 4.84 (after 120 min) were observed at 15°C, 20°C, 25°C, and 30°C, respectively.

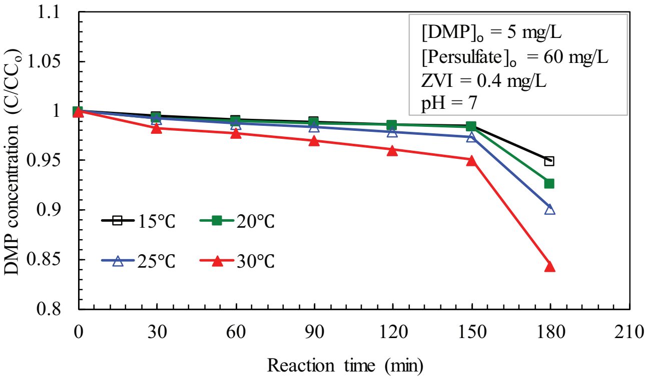

Fig. 8. Effect of reaction temperature on DMP degradation.

Degradation behaviors of DEHP, DBP, and DMP are compared at 15°C, 20°C, 25°C, and 30°C as shown in Figs. 11(a)–(d). Oxidation of PAEs in the ZVI-persulfate system occurred in the following order DBP > DEHP > DMP at lower temperature ranging from 15°C–20°C (Figs. 11(a) and (b)). Whereas, degradation rate of PAEs increased with increase in Carbon chain size at higher temperature conditions 25°C–30°C (Figs. 11(c) and (d)). DMP belongs to shortest carbon size chain PAE that was more resistive to degradation. Degradation of DBP was rapid during the first 30 min, after which degradation rate slowed down at all temperatures either because of the DBP adsorption on ZVI particles or because degradation rate depends on total DBP concentration present in the system. However, degradation rate of DEHP increased effectively with the increase in temperature as compare with DBP. Fe^{2+} release did not correlate well with the temperature increase potentially because our temperature range was relatively small. Maximum concentration of Fe^{2+} was observed at 30°C for batch tests with all three PAEs. Control samples exhibited < 4% losses due to evaporation.

4. Conclusions

Decomposition of three PAEs, DEHP, DBP, and DMP was explored under the presence of zero-valent iron and persulfate at different temperatures. Oxidation of persulfate ($S_2O_8^{2-}$) into sulfate (SO_4^{2-}), release of total dissolved iron and Fe^{2+} as well as pH fluctuation were also examined. All the batch reactions were conducted in 40 ml brown glass bottles, each of which initially contained 5 mg of each PAEs. Degradation of DEHP, DBP, and DMP at 15°C was equal to ~32%, 47%, and 5%, respectively. Degradation rate of PAEs at 15°C–20°C were

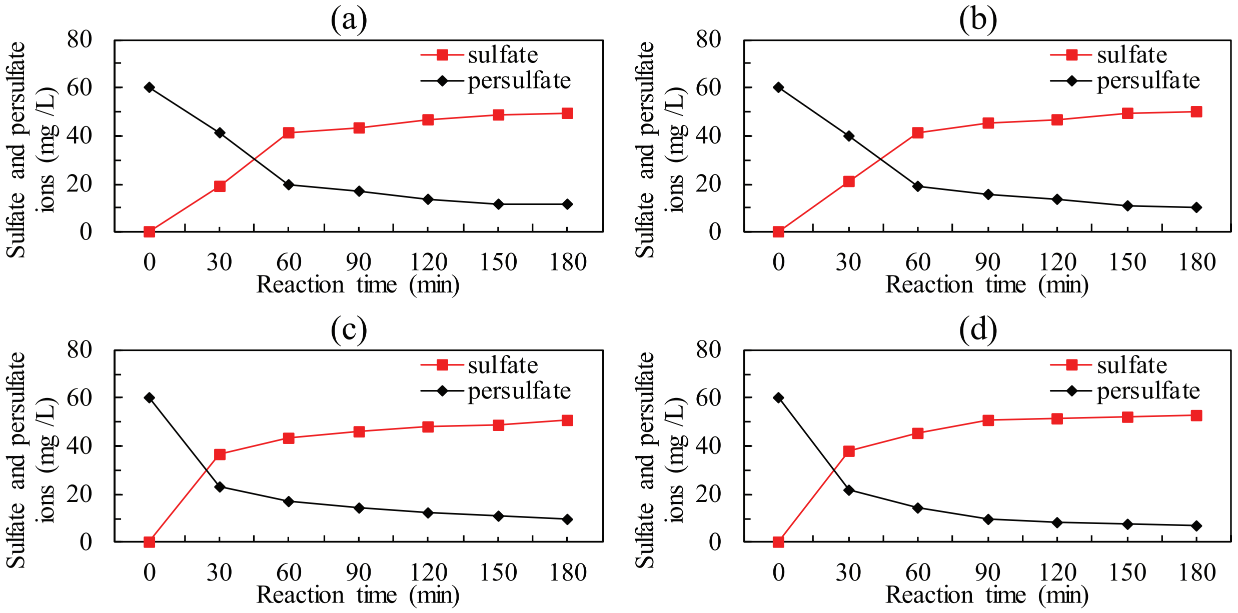

Fig. 9. Conversion of persulfate into sulfate during DMP tests at (a) 15°C, (b) 20°C, (c) 25°C, and (d) 30°C.

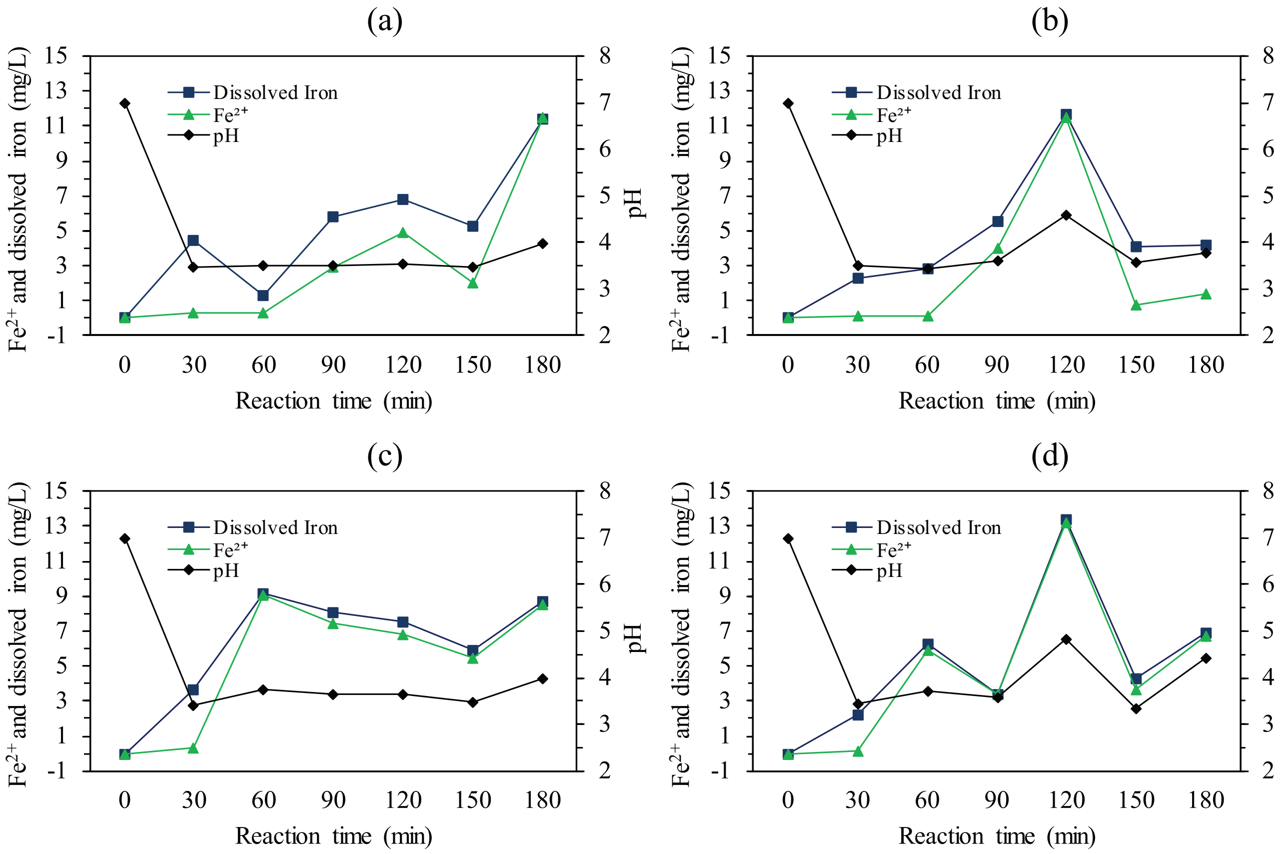

Fig. 10. Iron ions concentrations and pH during DMP decomposition at (a) 15°C, (b) 20°C, (c) 25°C, and (d) 30°C.

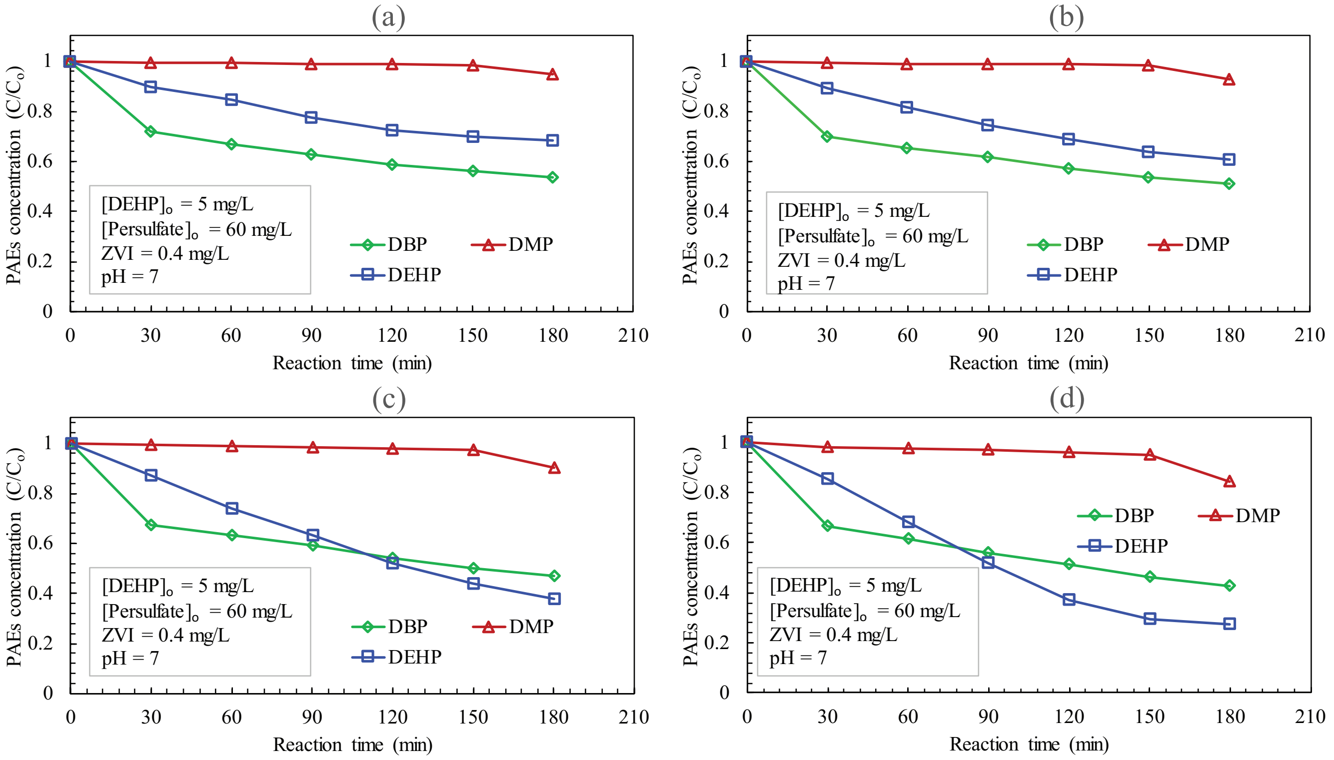

Fig. 11. Comparison of degradation of PAEs with carbon chains of different length (a) 15°C, (b) 20°C, (c) 25°C, and (d) 30°C.

in the following order: DBP > DEHP > DMP. Destruction of PAEs at 25°C–30°C was faster and more severe for PAEs with longer carbon chains. DBP destruction was the most efficient at all temperatures (15°C–30°C) in comparison with other two PAEs. Degradation rate of DEHP was significantly affected by temperature compared with DMP and DBP. Overall degradation of PAEs in ZVI-persulfate system was much faster comparing with other methods for in situ removal of PAEs from groundwater. Consumption of persulfate accelerated as temperature increased. Similarly, maximum concentration of Fe^{2+} was observed at 30°C: it was 11.46, 12.53, and 13.20 mg/L for batches containing DEHP, DBP, and DMP, respectively. pH values ranged from the 3.2–4.0. Our results clearly demonstrated that combination of ZVI and persulfate can effectively degrade PAEs under normal temperature range. Thus, it can be considered as a media for potential permeable reactive barriers for remediation of the sites contaminated with PAEs.

Acknowledgments

This study was supported by the National Natural Science Foundation of China (Grant No. 41572225), Beijing Natural Science Foundation (Grant No. 8181002) and Major Science and Technology Program for Water Pollution Control and Treatment (Grants No. 2018ZX07109-002 and 2009ZX07424-002). We would also like to thank the editor and anonymous reviewers for their valuable comments and suggestions to improve the quality of our paper.

Symbols

C_t – Concentration at time t, mg/L
C_O – Initial concentration, mg/L
CNEMC – China National Environmental Monitoring Centre
DEHP – Di(2-ethylhexyl) phthalate
DBP – Dibutyl phthalate
DMP – Dimethyl phthalate
HPLC – High performance liquid chromatography
PAE – Phthalic acid ester
PTFE – Polytetrafluoroethylene
$t_{1/2}$ – Half-life, min
US EPA – United States Environmental Protection Agency
WHO – World Health Organization
ZVI – Zero-Valent Iron

References

[1] F. Zeng, K. Cui, Z. Xie, L. Wu, D. Luo, L. Chen, Y. Lin, M. Liu, G. Sun, Distribution of phthalate esters in urban soils of subtropical city, Guangzhou, China, J. Hazard. Mater., 164 (2009) 1171–1178.

[2] Z. Xie, R. Ebinghaus, C. Temme, R. Lohmann, Caba, Armando, W. Ruck, Occurrence and air-sea exchange of phthalates in the Arctic, Environ. Sci. Tech., 41 (2007) 4555–4560.

[3] C.J. Weschler, T. Salthammer, H. Fromme, Partitioning of phthalates among the gas phase, airborne particles and settled dust in indoor environments, Atmos. Environ., 42 (2008) 1449–1460.

[4] Y. Guo, L. Wang, K. Kannan, Phthalates and parabens in personal care products from China: concentrations and human exposure, Arch. Environ. Contam. Toxicol., 66 (2014) 113–119.

[5] Y. Ji, F. Wang, L. Zhang, C. Shan, Z. Bai, Z. Sun, L. Liu, B. Shen, A comprehensive assessment of human exposure to phthalates from environmental media and food in Tianjin, China, J. Hazard. Mater., 279 (2014) 133–140.

[6] H. Liu, H. Liang, Y. Liang, D. Zhang, C. Wang, H. Cai, S.L. Shvartsev, Distribution of phthalate esters in alluvial sediment: a case study at JiangHan Plain, Central China, Chemosphere, 78 (2010) 382–388.

[7] B.R.T. Simoneit, P.M. Medeiros, B.M. Didyk, Combustion products of plastics as indicators for refuse burning in the atmosphere, Environ. Sci. Tech., 39 (2005) 6961–6970.

[8] B. Wang, H. Wang, W. Zhou, Y. Chen, Y. Zhou, Q. Jiang, Urinary excretion of phthalate metabolites in school children of China: implication for cumulative risk assessment of phthalate exposure, Environ. Sci. Tech., 49 (2015) 1120–1129.

[9] P. Du, Z. Zhou, H. Huang, S. Han, Z. Xu, Y. Bai, X. Li, Estimating population exposure to phthalate esters in major Chinese cities through wastewater-based epidemiology, Sci. Total Environ., 643 (2018) 1602–1609.

[10] X. Meng, Y. Wang, N. Xiang, L. Chen, Z. Liu, B. Wu, X. Dai, Y. Zhang, Z. Xie, R. Ebinghaus, Flow of sewage sludge-borne phthalate esters (PAEs) from human release to human intake: implication for risk assessment of sludge applied to soil, Sci. Total Environ., 476–477 (2014) 242–249.

[11] L. Niu, Y. Xu, C. Xu, L. Yun, W. Liu, Status of phthalate esters contamination in agricultural soils across China and associated health risks, Environ. Pollut., 195 (2014) 16–23.

[12] K. Huang, W. Chou, C. Wang, Y. Chang, C. Shu, Electrochemically assisted coagulation for the adsorptive removal of dimethyl phthalate from aqueous solutions using iron hydroxides, J. Taiwan. Inst. Chem. Eng., 50 (2015) 236–241.

[13] Y. Hongjun, X. Wenjun, L. Qing, L. Jingtao, Y. Hongwen, L. Zhaohua, Distribution of phthalate esters in topsoil: a case study in the Yellow River Delta, China, Environ. Monit. Assess., 185 (2013) 8489–8500.

[14] X. Zheng, B.T. Zhang, Y. Teng, Distribution of phthalate acid esters in lakes of Beijing and its relationship with anthropogenic activities, Sci. Total Environ., 476–477 (2014) 107–113.

[15] L. Chen, Y. Zhao, L. Li, B. Chen, Y. Zhang, Exposure assessment of phthalates in non-occupational populations in China, Sci. Total Environ., 427–428 (2012) 60–69.

[16] D. Gao, Z. Li, H. Wang, H. Liang, An overview of phthalate acid ester pollution in China over the last decade: environmental occurrence and human exposure, Sci. Total Environ., 645 (2018) 1400–1409.

[17] X. Liu, J. Shi, T. Bo, H. Zhang, W. Wu, Q. Chen, X. Zhan, Occurrence of phthalic acid esters in source waters: a nationwide survey in China during the period of 2009–2012, Environ. Pollut., 184 (2014) 262–270.

[18] K. Qi, Y. Xie, R. Wang, S-y. Liu, Z. Zhao, Electroless plating Ni-P cocatalyst decorated g-C_3N_4 with enhanced photocatalytic water splitting for H_2 generation, Appl. Surf. Sci., 466 (2019) 847–853.

[19] K. Qi, B. Cheng, J. Yu, W. Ho, Review on the improvement of the photocatalytic and antibacterial activities of ZnO, J. Alloys Compd., 727 (2017) 792–820.

[20] B. Yuan, X. Li, N. Graham, Reaction pathways of dimethyl phthalate degradation in TiO_2–UV–O_2 and TiO_2–UV–Fe(VI) systems, Chemosphere, 72 (2008) 197–204.

[21] G. Wen, J. Ma, Z.Q. Liu, L. Zhao, Ozonation kinetics for the degradation of phthalate esters in water and the reduction of toxicity in the process of O_3/H_2O_2, J. Hazard. Mater., 195 (2011) 371–377.

[22] T.K. Lau, W. Chu, N. Graham, The degradation of endocrine disruptor di-n-butyl phthalate by UV irradiation: a photolysis and product study, Chemosphere, 60 (2005) 1045–1053.

[23] L. Wang, G.Y. Fu, B. Zhao, Z. Zhang, X. Guo, H. Zhang, Degradation of di-n-butyl phthalate in aqueous solution by the O_3/UV process, Desal. Wat Treat., 52 (2014) 824–833.

[24] K.S. Tay, N.A. Rahman, M.R.B. Abas, Fenton degradation of dialkylphthalates: products and mechanism, Environ. Chem. Lett., 9 (2011) 539–546.

[25] R.J. Watts, A.L. Teel, Treatment of contaminated soils and groundwater using ISCO, Pract. Period. Hazard. Toxic Radioact. Waste Manage.t, 10 (2006) 2–9.

[26] G.H. Scott, E.P. Bruce, Engineering Issue Paper: in-situ chemical oxidation. EPA 600-R06-072, U.S. EPA, Office of Research and Development, Cincinnati, 2006.

[27] Kambhu, M. Gren, W. Tang, S. Comfort, C.E. Harris, Remediating 1,4-dioxane-contaminated water with slow-release persulfate and zerovalent iron, Chemosphere, 175 (2017) 170–177.

[28] Hussain, Y. Zhang, S. Huang, X. Du, Degradation of p-chloroaniline by persulfate activated with zero-valent iron, Chem. Eng. J., 203 (2012) 269–276.

[29] X. Wei, N. Gao, C. Li, Y. Deng, S. Zhou, L. Li, Zero-valent iron (ZVI) activation of persulfate (PS) for oxidation of bentazon in water, Chem. Eng. J., 285 (2016) 660–670.

[30] Y. Lu, X. Yang, L. Xu, Z. Wang, Y. Xu, G. Qian, Sulfate radicals from Fe3+/persulfate system for Rhodamine B degradation, Desal. Wat Treat., 57 (2016) 29411–29420.

[31] A.R. Zarei, H. Rezaeivahidian, A.R. Soleymani, Mineralization of unsymmetrical dimethylhydrazine (UDMH) via persulfate activated by zero valent iron nano particles: modeling, optimization and cost estimation, Desal. Wat Treat., 57 (2016) 16119–16128.

[32] Tsitonaki, B.G. Petri, M. Crimi, H. Mosbaek, R.L. Siegrist, P.L. Bjerg, In situ chemical oxidation of contaminated soil and groundwater using persulfate: a review, Crit. Rev. Env. Sci. Technol., 40 (2010) 55–91.

[33] M.G. Antoniou, A.A.D. La Cruz, D.D. Dionysiou, Degradation of microcystin-LR using sulfate radicals generated through photolysis, thermolysis and e− transfer mechanisms, Appl. Catal. B., 96 (2010) 290–298.

[34] J. Fang, C. Shang, Bromate formation from bromide oxidation by the UV/persulfate process, Environ. Sci. Technol., 46 (2012) 8976–8983.

[35] H. Li, J. Wan, Y. Ma, Y. Wang, M. Huang, Influence of particle size of zero-valent iron and dissolved silica on the reactivity of activated persulfate for degradation of acid orange 7, Chem. Eng. J., 237 (2014) 487–496.

[36] Z. Wang, D. Deng, L. Yang, Degradation of dimethyl phthalate in solutions and soil slurries by persulfate at ambient temperature, J. Hazard. Mater., 271 (2014) 202–209.

[37] H. Li, J. Wan, Y. Ma, M. Huang, Y. Wang, Y. Chen, New insights into the role of zero-valent iron surface oxidation layers in persulfate oxidation of dibutyl phthalate solutions, Chem. Eng. J., 250 (2014) 137–147.

[38] C. Liang, C. Huang, N. Mohanty, R.M. Kurakalva, A rapid spectrophotometric determination of persulfate anion in ISCO, Chemosphere, 73 (2008) 1540–1543.

[39] S.Y. Oh, H.W. Kim, J.M. Park, H.S. Park, C. Yoon, Oxidation of polyvinyl alcohol by persulfate activated with heat, Fe^{2+}, and zero-valent iron, J. Hazard. Mater., 168 (2009) 346–351.

[40] Ghauch, G. Ayoub, S. Naim, Degradation of sulfamethoxazole by persulfate assisted micrometric Fe0 in aqueous solution, Chem. Eng. J., 228 (2013) 1168–1181.

[41] D.H. Bremner, A.E. Burgess, D. Houllemare, K. Namkung, Phenol degradation using hydroxyl radicals generated from zero-valent iron and hydrogen peroxide, Appl. Catal. B., 63 (2006) 15–19.